

THE LOW QUIESCENT X-RAY LUMINOSITY OF THE NEUTRON STAR TRANSIENT XTE J2123–058

JOHN A. TOMSICK¹, DAWN M. GELINO¹, JULES P. HALPERN², PHILIP KAARET³

Draft version November 18, 2018

ABSTRACT

We report on the first X-ray observations of the neutron star soft X-ray transient (SXT) XTE J2123–058 in quiescence, made by the *Chandra X-ray Observatory* and *BeppoSAX*, as well as contemporaneous optical observations. In 2002, the *Chandra* spectrum of XTE J2123–058 is consistent with a power-law model, or the combination of a blackbody plus a power-law, but it is not well-described by a pure blackbody. Using the interstellar value of N_{H} , the power-law fit gives $\Gamma = 3.1_{-0.6}^{+0.7}$ and indicates a 0.3–8 keV unabsorbed luminosity of $(9_{-3}^{+4}) \times 10^{31} (d/8.5 \text{ kpc})^2 \text{ ergs s}^{-1}$ (90% confidence errors). Fits with models consisting of thermal plus power-law components indicate that the upper limit on the temperature of a $1.4 M_{\odot}$, 10 km radius neutron star with a hydrogen atmosphere is $kT_{\text{eff}} < 66 \text{ eV}$, and the upper limit on the unabsorbed, bolometric luminosity is $L_{\infty} < 1.4 \times 10^{32} \text{ ergs s}^{-1}$, assuming $d = 8.5 \text{ kpc}$. Of the neutron star SXTs that exhibit short (< 1 year) outbursts, including Aql X-1, 4U 1608–522, Cen X-4, and SAX J1810.8–2609, the lowest temperatures and luminosities are found for XTE J2123–058 and SAX J1810.8–2609. From the *BeppoSAX* observation of XTE J2123–058 in 2000, we obtained an upper limit on the 1–10 keV unabsorbed luminosity of $9 \times 10^{32} \text{ ergs s}^{-1}$. Although this upper limit allows that the X-ray luminosity may have decreased between 2000 and 2002, that possibility is not supported by our contemporaneous *R*-band observations, which indicate that the optical flux increased significantly. Motivated by the theory of deep crustal heating by Brown and co-workers, we characterize the outburst histories of the five SXTs. The low quiescent luminosity for XTE J2123–058 is consistent with the theory of deep crustal heating without requiring enhanced neutron star cooling if the outburst recurrence time is $\gtrsim 70$ years.

Subject headings: accretion, accretion disks — stars: individual (XTE J2123–058, SAX J1810.8–2609) — stars: neutron — X-rays: stars

1. INTRODUCTION

Accreting neutron stars can be found in high-mass (HMXB) or low-mass (LMXB) X-ray binary systems. The majority of HMXBs have transient X-ray emission. Their outburst spectra are relatively hard and X-ray pulsations from these highly magnetized ($B \sim 10^{12} \text{ G}$) neutron stars are typically detected. A wide variety of X-ray behaviors are seen for neutron star LMXBs, but, in general, the lack of X-ray pulsations from most (but not all) of these systems, and the emission of type I X-ray bursts from some, suggest that they harbor neutron stars with relatively low magnetic field strengths ($B \sim 10^{8-9} \text{ G}$). During ≈ 33 years of X-ray observations, some sources (e.g., Sco X-1, Cyg X-2) have maintained luminosities approaching the Eddington limit of $\approx 10^{38} \text{ ergs s}^{-1}$, while others are able to maintain persistent luminosities several orders of magnitude lower (Wilson et al. 2003). In addition, there is a class of transient neutron star LMXBs for which the luminosity varies from a substantial fraction of Eddington to quiescent levels typically near $10^{32-33} \text{ ergs s}^{-1}$. In outburst, these systems have relatively soft spectra compared to the HMXBs, and are commonly grouped with black hole transients as soft X-ray transients (SXTs).

In quiescence, most neutron star SXTs exhibit X-ray energy spectra with a component that is typically fitted well by a blackbody, suggesting that the origin of this compo-

nent is thermal emission from the surface of a cooling neutron star. Although a pure blackbody often provides a good fit to the spectrum, unphysical neutron star radii near 1 km are inferred unless an atmosphere is modeled (Rutledge et al. 1999). In addition to the thermal component, the energy spectra often contain a second component that has a power-law shape. The brightest and best studied systems in this class, Cen X-4 and Aql X-1, usually display both components (Rutledge et al. 2001, 2002a; Campana & Stella 2003; Campana et al. 2004). However, other systems may be dominated by the thermal component, such as MXB 1659–29 (Wijnands et al. 2003b) and sources X-5 and X-7 in the globular cluster 47 Tucanae (Heinke et al. 2003), or by the power-law component, such as SAX J1808.4–3658 (Campana et al. 2002) and EXO 1745–248 (Wijnands et al. 2003a). Although theories for the thermal component, such as the deep crustal heating model of Brown, Bildsten & Rutledge (1998), are relatively well-developed and are being tested with observations, the origin of the power-law component is not understood beyond suggestions that it may be related to accretion onto the neutron star magnetosphere (Campana et al. 1998) or a putative pulsar wind colliding with infalling matter from the companion star (Tavani 1991). In addition to our lack of understanding of the power-law component, questions remain about the mass accretion rate in quiescence, the origin of rapid (100–10,000 s) variability (Rutledge et al. 2002a; Campana et al. 2004), and the origin of variability in the thermal component on longer time scales (Rutledge et al. 2002a). Another important question is if quiescent observational properties correlate with other known differences between neutron star SXTs, such as whether they are millisecond X-ray pulsars (during outbursts) or not, whether the systems are in the field

¹ Center for Astrophysics and Space Sciences, Code 0424, University of California at San Diego, La Jolla, CA, 92093, USA (e-mail: jtom-sick@ucsd.edu)

² Columbia Astrophysics Laboratory, Columbia University, 550 West 120th Street, New York, NY 10027

³ Harvard-Smithsonian Center for Astrophysics, 60 Garden Street, Cambridge, MA, 02138, USA

or in globular clusters, and whether their X-ray outbursts are long (years to decades) or short (weeks to months).

Here, we report on X-ray and optical observations of the field neutron star SXT XTE J2123–058 taken during quiescence. XTE J2123–058 had its only detected X-ray outburst in 1998 June–August (Levine, Swank & Smith 1998; Tomsick et al. 1999), and we focus on observations made with *Chandra*, *BeppoSAX*, and optical telescopes 2–4 years after the outburst. During the outburst, the *Rossini X-ray Timing Explorer (RXTE)* detected type I X-ray bursts and a pair of kHz quasi-periodic oscillations (Homan et al. 1999; Tomsick et al. 1999), indicating that the system contains a rapidly rotating neutron star. However, coherent X-ray pulsations were not found. The 6 hr binary orbital period and the fact that the binary inclination of the system is relatively high were established from optical modulation and the presence of partial eclipses in the optical light curve (Tomsick et al. 1999; Soria, Wu & Galloway 1999; Zurita et al. 2000; Shahbaz et al. 2003). The high Galactic latitude ($b = -36^\circ$) and low extinction have allowed for detailed optical studies of XTE J2123–058 in quiescence even though the source is rather faint at its relatively large distance (8.5 ± 2.5 kpc). The optical observations show that XTE J2123–058 consists of a K7 V star on or close to the main sequence and a neutron star for which mass determinations of $1.5 \pm 0.3 M_\odot$ (Tomsick et al. 2001; Casares et al. 2002; Tomsick et al. 2002) and $1.04\text{--}1.56 M_\odot$ (Shahbaz et al. 2003) have been obtained. The focus of this paper is the first X-ray study of XTE J2123–058 in quiescence.

2. OBSERVATIONS AND ANALYSIS

We observed XTE J2123–058 with *Chandra* on UT 2002 November 13 (ObsID 2709), using the Advanced CCD Imaging Spectrometer (ACIS) with the target placed on one of the back-illuminated ACIS chips (ACIS-S3). For our analysis, we used the “level 2” event list produced by the standard data processing with ASCDS version 6.9.2 using Calibration Data Base (CALDB) version 2.17. Light curves using counts from the full field-of-view do not show any background flares, allowing us to use the data from the full 17,706 s integration. Using the *Chandra* Interactive Analysis of Observations (CIAO) version 3.0 software routine *wavdetect* (Freeman et al. 2002), we searched for sources on the S3 chip in the 0.3–8 keV energy band. We detected 22 sources with counts between 5 and 108 per source, using a detection threshold of 10^{-6} , including a 24 count source at R.A. = $21^{\text{h}}23^{\text{m}}14^{\text{s}}.54$, decl. = $-05^\circ47'53''.2$ (equinox J2000, uncertainty $0''.6$). This position is consistent with the target’s optical position (Tomsick et al. 1999), and we conclude that this source is the quiescent X-ray counterpart of XTE J2123–058.

We also report on a *BeppoSAX* observation of the XTE J2123–058 field made on UT 2000 May 12–13. We produced 1–10 keV images using the data from the two Medium Energy Concentrator/Spectrometer (MECS) units that were operational during the observation (units 2 and 3). We also produced a 0.1–10 keV image using data from the Low Energy Concentrator/Spectrometer (LECS). We obtained a MECS exposure time of 46,340 s and a LECS exposure time of 17,080 s. To search for sources, we convolved each of the three images with a two-dimensional Gaussian with a width (σ) of 5 pixels ($40''$) in both directions. Only one source was clearly detected in both of the MECS images at R.A. = $21^{\text{h}}22^{\text{m}}50^{\text{s}}.6$, decl. = $-05^\circ45'09''$ (equinox J2000, uncertainty

$\sim 1'$), and this source, which we call SAX J2122.8–0575, is also present in the LECS image. It is clear that SAX J2122.8–0575 is not XTE J2123–058 as they are separated by $6'.6$. We conclude that XTE J2123–058 was not detected during the *BeppoSAX* observation, and we derive an upper limit on its X-ray flux below.

Finally, we obtained *R*-band images on three occasions close to the times of the X-ray observations. As shown in Table 1, we observed XTE J2123–058 using the 2.4 m Hiltner telescope of the MDM Observatory on 2000 July 24, about 2 months after the *BeppoSAX* observation. We also observed XTE J2123–058 with the Shane 3 m telescope of Lick Observatory about 2 months before the *Chandra* observation and again at MDM about 2 weeks after the *Chandra* observation. For both MDM runs, we used the same SITE 2048 \times 2048 pixel, thinned, back-illuminated CCD with a spatial scale of $0''.275$ per $24 \mu\text{m}$ pixel, and an *R* filter that is very close to Harris *R*.⁴ At Lick, we used the Prime Focus Camera, with a SITE 2048 \times 2048 pixel, thinned CCD with a spatial scale of $0''.296$ per $24 \mu\text{m}$ pixel, and a Kron-Cousins *R* filter. In all, we obtained thirteen 600–700 s exposures (see Table 1), and we reduced the images using standard IRAF⁵ routines. For XTE J2123–058, we carried out the photometry with the IRAF package *phot* and used two calibrated reference stars with *R* magnitudes of 19.47 and 19.51. In 2002, the conditions at Lick were photometric, and we observed Landolt (1992) standards to obtain the calibration. We note that this calibration is about 0.1 magnitudes brighter than the calibration previously obtained using MDM observations from 1998 reported in Tomsick et al. (1999).

3. ENERGY SPECTRUM AND SOURCE LUMINOSITY

We used the CIAO software routine *psextract* to produce the ACIS energy spectrum for XTE J2123–058 and to create the appropriate instrument response matrix for the spectrum. The software used CALDB 2.23 to create the response matrix, and we included a correction for the time-dependence of the ACIS response. The source spectrum included counts from a circular region with a 5 pixel (about $2''.5$) radius, and we estimated the background level using counts from a source-free annulus around the target position. The source spectrum consists of 24 counts, and we estimate a background level of 0.7 counts in the extraction region. We produced a “light curve” of the source in six time bins of ≈ 3000 s. Each bin contains between 2 and 6 counts, which is consistent with a constant flux; however, the low count rate does not allow us to place tight constraints on the possible amplitude of variability. The small number of counts also indicates that χ^2 statistics are not appropriate for spectral analysis, as the assumption of a Gaussian probability distribution in each spectral bin is not met. Thus, we carried out our spectral analysis by minimizing the Cash statistic (Cash 1979), which is appropriate in cases where the assumption of a Poisson probability distribution in each spectral bin is valid. We fitted the spectrum using XSPEC 11.2.

The spectra of other neutron star SXTs are typically well-described by a blackbody, a power-law, or both components with interstellar absorption. We began by fitting the spec-

⁴ See <http://www.astro.lsa.umich.edu/obs/mdm/technical/filters> for the exact transmission curve.

⁵ IRAF (Image Reduction and Analysis Facility) is distributed by the National Optical Astronomy Observatories, which are operated by the Association of Universities for Research in Astronomy, Inc., under cooperative agreement with the National Science Foundation.

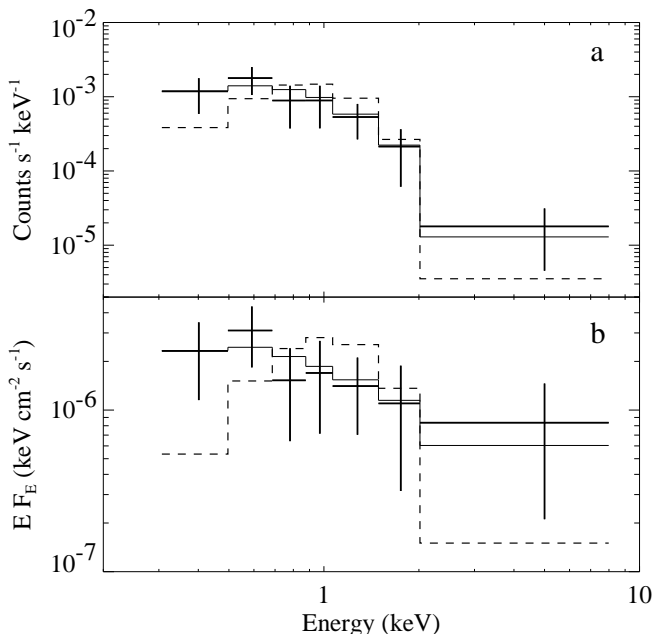


FIG. 1.— *Chandra*/ACIS energy spectrum of XTE J2123–058. *Top*: folded through the detector response. *Bottom*: unfolded. In each panel, the *solid line* is a power-law fit to the data (using Cash statistics as described in the text) with N_{H} fixed at the interstellar value. The power-law photon index is $3.1^{+0.7}_{-0.6}$, and the unabsorbed 0.3–8 keV luminosity is $(9^{+4}_{-3}) \times 10^{31}$ ergs s^{-1} . A blackbody model (*dashed line*), by itself, does not provide a good description of the spectrum.

trum for XTE J2123–058 with an absorbed power-law, and the results are given in Table 2. Once we found the best-fitted parameters by minimizing the Cash statistic, we determined the quality of the fit and the 90% confidence errors on the parameters by producing and fitting 10,000 simulated spectra. We used the best-fitted parameters from the fits to the actual data as input to the simulations. Using simulations to determine the parameter errors is necessary only because of the small number of counts in the spectrum. We tested our method by producing spectra with 2–3 times as many counts, and we found that the errors produced by calculating changes in the Cash statistic (the standard technique) match the values we obtain using simulations. In addition to the power-law model, we used simulations to determine the errors on parameter for all other fits presented in this work. For the power-law model, we obtain $N_{\text{H}} = (7.0^{+40.0}_{-7.0}) \times 10^{20}$ cm^{-2} for the column density and $\Gamma = 3.1^{+2.8}_{-0.8}$ for the photon index. The fit using a blackbody model is significantly worse than the power-law model as indicated by the fact that for 97% of the simulated spectra we obtained a better Cash statistic than the one obtained when fitting the actual spectrum (compared to 69% for the power-law model).

We refitted the spectrum with the same spectral models but with N_{H} fixed to the interstellar column density. The interstellar N_{H} comes from the A_V measurement of Hynes et al. (2001), which gives $N_{\text{H}} = (6.6 \pm 2.7) \times 10^{20}$ cm^{-2} , and the total Galactic H I value of 5.7×10^{20} cm^{-2} from Dickey & Lockman (1990). We adopt a value of 6×10^{20} cm^{-2} . For the power-law alone, we obtain $\Gamma = 3.1^{+0.7}_{-0.6}$ and an unabsorbed 0.3–8 keV flux of $(1.1^{+0.5}_{-0.4}) \times 10^{-14}$ ergs cm^{-2} s^{-1} ,

which corresponds to a luminosity of $(9^{+4}_{-3}) \times 10^{31}$ ergs s^{-1} at a distance of 8.5 kpc. The best fitted blackbody temperature is 240^{+60}_{-50} eV, but the quality of the blackbody fit is even worse (98.7%) with N_{H} fixed. Figure 1 shows the spectrum (rebinned for clarity, although the Cash fits are performed without rebinning) along with the best fitted power-law and blackbody models with N_{H} fixed. It is clear that the curvature of the blackbody model is too large, underpredicting the observed spectrum below 0.7 keV and above 2 keV. This, along with the measurements of the fit quality from the simulations, indicates that the spectrum is well-described by a power-law model or the combination of a blackbody and a power-law model, but it is not well-described by a blackbody alone.

Although a power-law alone provides an adequate description of the ACIS spectrum, we performed additional fits to obtain limits on the temperature and luminosity of the putative thermal component that is expected to be emitted from the surface of the neutron star. We fitted the spectrum with a model consisting of a power-law component along with thermal emission from an atmosphere composed of hydrogen. The latter component was modeled using the “Neutron Star Atmosphere” (NSA) model of Zavlin, Pavlov & Shibano (1996). We assumed a neutron star mass of $1.4 M_{\odot}$, which is consistent with the measured mass, and a radius of 10 km. With these parameters fixed, the remaining free parameters in the NSA model are the temperature (kT_{eff}) and the distance. For XTE J2123–058, there are several arguments that lead to distance estimates in the range 5–15 kpc (Tomsick et al. 1999; Homan et al. 1999; Zurita et al. 2000), but the most reliable estimates come from optical observations of the source in quiescence. Previous estimates include 8 ± 3 kpc (Zurita et al. 2000), 8.5 ± 2.5 kpc (Tomsick et al. 2001), and 9.6 ± 1.3 kpc (Casares et al. 2002). Here, we adopt a range of 6–11 kpc. We performed the NSA plus power-law fits with the distance fixed to three values spanning this range (6, 8.5, and 11 kpc). As shown in Table 3, the 90% confidence upper limits on kT_{eff} are 57, 66, and 73 eV, respectively, for these three distances. Using $L_{\infty} = 4\pi R^2 \sigma T_{\text{eff}}^4 (1 - 2GM/Rc^2)$, where $R = 10$ km and $M = 1.4 M_{\odot}$, upper limits on the unabsorbed luminosity from the NSA component as seen by a distant observer are 8.0×10^{31} , 1.4×10^{32} and 2.1×10^{32} ergs s^{-1} for distances of 6, 8.5, and 11 kpc, respectively. While these values are bolometric luminosities, it should be noted that we cannot rule out the possibility that there is thermal emission at energies below the *Chandra* bandpass.

Although XTE J2123–058 was not detected by *BeppoSAX* in 2000 May, we can calculate upper limits on its luminosity if we assume that the energy spectrum was similar to that measured by *Chandra*. To calculate the upper limits, we assume the simplest model of an absorbed power-law with a photon index of 3.1 and the interstellar column density. For the MECS (units 2 and 3 combined), we measure a 1–10 keV count rate of 1.684 ks^{-1} in a circle of radius $2'$ centered on the XTE J2123–058 position. This is not significantly higher than the expected background rate (using a blank-sky pointing) of 1.675 ks^{-1} . These values imply a $3\text{-}\sigma$ upper limit on the count rate from XTE J2123–058 of 0.676 ks^{-1} , which corresponds to an unabsorbed flux $< 1.02 \times 10^{-13}$ ergs cm^{-2} s^{-1} , and a 1–10 keV luminosity $< 9 \times 10^{32}$ ergs s^{-1} for $d = 8.5$ kpc. For the LECS, the 0.1–1 keV count rate in a $2'$ radius circle centered on XTE J2123–058 is 1.230 ks^{-1} , which is actually somewhat lower than the expected background rate of 1.466 ks^{-1} . Using the expected background rate, the $3\text{-}\sigma$ upper limit on the unabsorbed 0.1–1 keV flux is 1.75×10^{-12} ergs cm^{-2} s^{-1} , corre-

sponding to a luminosity $< 1.5 \times 10^{34}$ ergs s^{-1} for $d = 8.5$ kpc.

4. OPTICAL RESULTS

Figure 2 shows the R magnitudes for XTE J2123–058 from three exposures taken in 2000 July at MDM, two exposures taken in 2002 September at Lick, and eight exposures taken in 2002 November at MDM. Previously, Shahbaz et al. (2003) reported on extensive R -band photometry of XTE J2123–058 taken between 1999 June and 2000 August. The R -band light curve was relatively stable at that time, showing orbital ellipsoidal modulations with a peak-to-peak amplitude of about 0.25 magnitudes. The dashed lines in Figure 2 indicate the range of the modulation in 1999–2000, which was $21.70 < R < 21.95$. While our 2000 May measurements of 21.63 ± 0.07 , 21.75 ± 0.08 , and 21.57 ± 0.07 are consistent with the brighter end of this range, our later observations indicate that XTE J2123–058 brightened between 2000 and 2002. The range of R between 21.41 ± 0.07 and 21.01 ± 0.03 over 25% of the 6 hr binary orbital period during the 2002 November run indicates that the source continues to vary, but with a peak level that is at least 0.6–0.7 magnitudes brighter than the peak level of $R = 21.7$ measured by Shahbaz et al. (2003). As our observations do not cover the full binary orbit, it is not clear whether this change is due to the addition of a constant component to the light curve or if the shape of the modulations has changed. Although it would be useful to know the orbital phases corresponding to the 2002 data, the binary ephemeris is too uncertain to extrapolate to 2002 as discussed in Tomsick et al. (2002). In the future, it may be worthwhile to obtain an X-ray observation while measuring the optical or IR light curve for a full 6 hr binary orbit.

As we are reporting the first sensitive X-ray observations of XTE J2123–058 in quiescence, comparison can be made with a prior prediction for the quiescent X-ray luminosity of this source that was made by modeling quiescent R -band light curves in 1999 and 2000. Shahbaz et al. (2003) predicted an X-ray luminosity of $\sim 10^{33}$ ergs s^{-1} , which is only slightly higher than our upper limit from the *BeppoSAX* observation made in 2000, but an order of magnitude higher than we observed with *Chandra* in 2002. While the X-ray observations would allow for the possibility that the quiescent X-ray luminosity decreased significantly between 2000 and 2002, our optical observations made in 2000 and 2002 indicate that the R -band flux actually increased over this time. If the 2000 R -band light curve showed a significant contribution from X-ray heating, it is difficult to see how a drop in X-ray flux could lead to an increase in the optical, thus, it is possible that Shahbaz et al. (2003) over-estimated the contribution from X-ray heating.

5. INTERPRETATION

X-ray observations of neutron star SXTs in quiescence provide tests of theoretical models for the thermal component. According to the theory of deep crustal heating by Brown, Bildsten & Rutledge (1998), the temperature of the neutron star core is maintained by nuclear reactions in the deep crust that occur when the mass accretion rate is high during outburst. As the thermal time scale for the core is $\sim 10,000$ years (Colpi et al. 2001), the level of quiescent thermal emission is set by the average mass accretion rate over this time span according to $L_q = 9 \times 10^{32} \langle \dot{M} \rangle_{-11}$ ergs s^{-1} (see Equation 1 of Rutledge et al. 2002b), assuming 1.45 MeV of heat deposited in the crust per accreted nucleon (Haensel & Zdunik 1990). Here $\langle \dot{M} \rangle_{-11}$ is

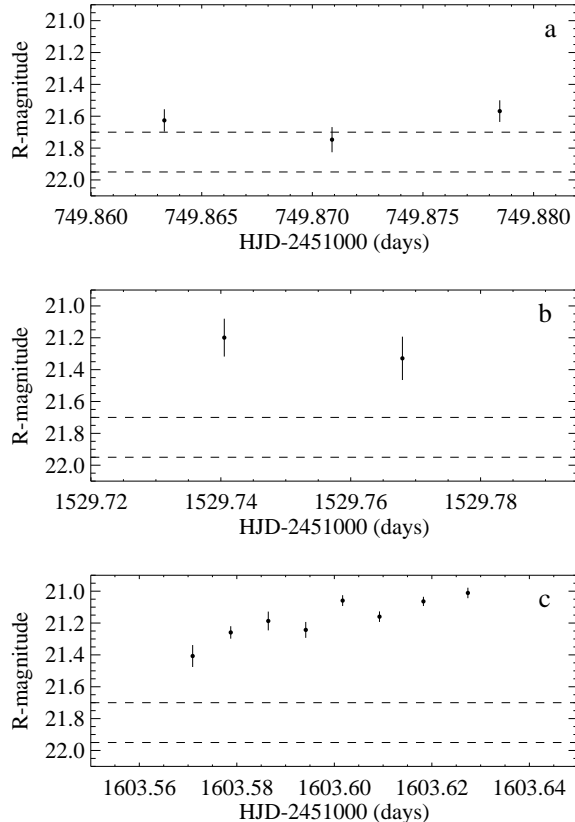


FIG. 2.— R -band measurements of XTE J2123–058. (a) 2000 July at MDM Observatory. (b) 2002 September at Lick Observatory. (c) 2002 November at MDM Observatory. The dashed lines delimit the levels measured by Shahbaz et al. (2003) during 1999–2000. An increase in the R -band flux between 2000 and 2002 is apparent.

the mass accretion rate averaged over the thermal time scale of the core in units of $10^{-11} M_{\odot} \text{ yr}^{-1}$, and L_q is the quiescent bolometric luminosity. While the time-averaged mass accretion rate is only a predictor of L_q if the neutron star core has reached thermal equilibrium, the lifetimes of LMXB systems are much longer than the thermal time scale of the core, and it is expected that thermal equilibrium has been established for all or nearly all of the LMXBs. While the long thermal time scale for the core precludes appreciable changes in the core temperature during a single SXT outburst, the neutron star crust can be heated significantly for the systems with longer outbursts (years to decades) so that the quiescent emission is determined by the evolution of the physical conditions in the crust (Rutledge et al. 2002b). However, for the systems with shorter outbursts (weeks to months), the properties of the quiescent thermal emission are primarily set by the conditions in the neutron star core (Brown, Bildsten & Rutledge 1998).

For a system like XTE J2123–058 that has undergone one ≈ 40 day outburst, the deep crustal heating theory implies that quiescent thermal emission provides information about the neutron star core. Here, we compare the quiescent properties of XTE J2123–058 to similar systems. The comparison group includes field neutron star SXTs with outbursts lasting less than 1 year for which quiescent X-ray observations have been reported. We only consider LMXB systems

from which X-ray bursts have been detected, proving that the accreting object is a neutron star. We restrict the comparison group to field systems because the outburst histories for most transients in globular clusters are uncertain due to source confusion in instruments with angular resolution worse than *Chandra*. Thus, our comparison group consists of the neutron star SXTs Aql X-1, 4U 1608–522, Cen X-4, and SAX J1810.8–2609. We also compare the quiescent properties of XTE J2123–058 to those of the millisecond X-ray pulsar SAX J1808.8–3658 as the quiescent X-ray luminosities of the two sources are comparable.

Table 4 compares the parameters of the thermal component for the five systems, including kT_{eff} , R , L_{∞} , and the gravitational redshift parameter, $g = \sqrt{1 - 2GM/Rc^2}$, assuming that all the neutron star masses are $1.4M_{\odot}$. For the spectral fits to XTE J2123–058, we set $R = 10$ km, and Jonker, Wijnands & van der Klis (2004) make the same assumption for SAX J1810.8–2609. However, for the other sources, we use the best fitted radii, and the parameters are taken from Rutledge et al. (1999, 2001, 2002a). The thermal component is detected for Cen X-4, Aql X-1, and 4U 1608–522, and a power-law component is also required for Cen X-4 and for some of the observations of Aql X-1. For XTE J2123–058 and SAX J1810.8–2609, the thermal component is not statistically required, and we report upper limits on the thermal component parameters for these two systems. Also, for all the sources we assume the best current distance measurement. The temperature upper limits for XTE J2123–058 (66 eV) and SAX J1810.8–2609 (72 eV) are about a factor of 2.5 lower than the 4U 1608–522 measurement of 170 eV, and the luminosity upper limits for XTE J2123–058 and SAX J1810.8–2609 are about a factor of 50 lower than the maximum quiescent luminosity measured for Aql X-1. The temperature and luminosity of Cen X-4 are intermediate between the hottest and most luminous sources (Aql X-1 and 4U 1608–522) and the coolest and least luminous sources (XTE J2123–058 and SAX J1810.8–2609).

Here, we characterize the outburst histories of these five sources to determine if they are related to the quiescent thermal properties as is expected in the Brown, Bildsten & Rutledge (1998) theory. From a review of SXT light curves covering the time period between 1969 and 1996 (Chen, Shrader & Livio 1997) and the *RXTE* All-Sky Monitor (ASM) covering 1996 to 2003, 4U 1608–522 had 16 outbursts with a mean peak X-ray luminosity, \bar{L}_{peak} , of $2.5 \times 10^{37} (d/3.6 \text{ kpc})^2 \text{ ergs s}^{-1}$. Aql X-1 had 21 outbursts with $\bar{L}_{\text{peak}} = 3.6 \times 10^{37} (d/5 \text{ kpc})^2 \text{ ergs s}^{-1}$. Cen X-4 had two outbursts (in 1969 and 1979) with $\bar{L}_{\text{peak}} = 5.6 \times 10^{37} (d/1.2 \text{ kpc})^2 \text{ ergs s}^{-1}$, and XTE J2123–058 had one outburst (in 1998) with $\bar{L}_{\text{peak}} = 1.7 \times 10^{37} (d/8.5 \text{ kpc})^2 \text{ ergs s}^{-1}$. Like XTE J2123–058, SAX J1810.8–2609 had only one outburst, also in 1998.

SAX J1810.8–2609 was discovered by Natalucci et al. (2000); and the only reported X-ray detections of this source in outburst were from *BeppoSAX* and *ROSAT* in 1998 March (Natalucci et al. 2000; Greiner et al. 1999). However, the ASM light curve shown in Figure 3c indicates that SAX J1810.8–2609 was in outburst by 1998 January 4 (MJD 50,817) and probably as early as 1997 December 18 (MJD 50,800). The dashed lines in Figure 3c mark the times of the *BeppoSAX* discovery at MJD 50,882–50,885 and the *ROSAT* observation at MJD 50,896, while it is clear that the source was considerably brighter prior to this. From

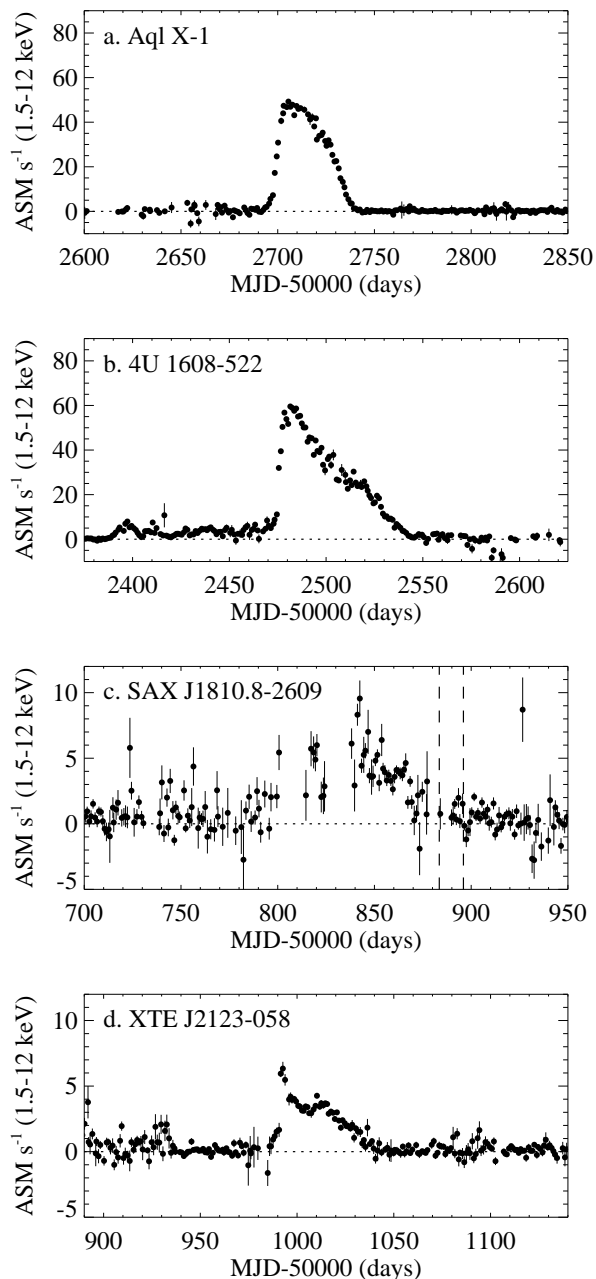


FIG. 3.— All-Sky Monitor (ASM) light curves for the four neutron star SXTs in our comparison group that had outbursts during the *RXTE* lifetime. Each point represents the average ASM count rate over 1 day. One Crab flux equals 75 ASM counts s^{-1} . For SAX J1810.8–2609 (c), the vertical dashed lines mark the times of previously reported *BeppoSAX* and *ROSAT* observations. Aql X-1 and 4U 1608–522 have had many outbursts during the lifetime of *RXTE*, and the light curves in (a) and (b) are representative.

the 1.5–12 keV ASM light curve, $\bar{L}_{\text{peak}} = 1.0 \times 10^{37} (d/4.9 \text{ kpc})^2 \text{ ergs s}^{-1}$. Although it has been suggested that SAX J1810.8–2609 had an unusually low outburst luminosity (Jonker, Wijnands & van der Klis 2004), the value we derive from the ASM measurements is comparable to the other neutron star SXTs. Figure 3 also shows the ASM light curve for the XTE J2123–058 outburst as well as sample outburst light curves for Aql X-1 and 4U 1608–522 (Cen X-4 has not

had an outburst during the *RXTE* lifetime). These light curves demonstrate that individual outbursts from different sources are similar in duration (typically 40–80 days) and overall shape, although it should be noted that exceptional outbursts do occur (Chen, Shrader & Livio 1997).

For each of the neutron star SXTs, the time-averaged mass accretion rate over the past 33 years can be expressed as

$$\langle \dot{M} \rangle = \frac{\bar{L}_{\text{peak}} N t_{\text{outburst}} f}{\epsilon c^2 (33 \text{yr})} = s \bar{L}_{\text{peak}} N, \quad (1)$$

where N is the number of outbursts, t_{outburst} is the typical duration of an outburst from the source, f is a factor with a value less than 1.0 that accounts for the shape of the outburst light curve, ϵ is the fraction of the rest mass energy released from accreted matter, and $s = t_{\text{outburst}} f / \epsilon c^2 (33 \text{yr})$. As the durations and light curve shapes are similar for the sources in our comparison group, s is approximately the same for these sources, and the time-averaged mass accretion rate over the past 33 years is proportional to $\bar{L}_{\text{peak}} N$. We estimate s using $t_{\text{outburst}} = 60$ days and $\epsilon = 0.2$, which is the value of ϵ that is typically assumed for accretion onto a neutron star (Rutledge et al. 2002b). Although the precise value of f depends on the exact shape of the outburst light curve, it can be approximated as the mean outburst flux divided by the peak flux. For the XTE J2123–058 ASM light curve, the mean flux over a 60 day period that includes the 1998 outburst is 41% of the peak level, and we use $f = 0.4$, giving $s = 1.1 \times 10^{-23} \text{ s}^2 \text{ cm}^{-2}$. Using this value of s for all five sources and the values for \bar{L}_{peak} and the number of outbursts (N) given above, we calculate estimates of the time-averaged mass accretion rate over the past 33 years. The values for $\langle \dot{M} \rangle$ are given in Table 4, and they show that this quantity is a relatively good predictor of L_{∞} . Aql X-1 and 4U 1608–522 have the highest values of both $\langle \dot{M} \rangle$ and L_{∞} , XTE J2123–058 and SAX J1810.8–2609 have the lowest, and Cen X-4 is intermediate. The ratio of the value of $\langle \dot{M} \rangle$ for Aql X-1 to that for XTE J2123–058 is 45, which is consistent with their ratio of L_{∞} , which is > 38 . Similarly, the Aql X-1 to SAX J1810.8–2609 ratio of $\langle \dot{M} \rangle$ is 76, and this is consistent with their ratio of L_{∞} , which is > 27 . While these measurements are in line with the Brown, Bildsten & Rutledge (1998) theory, a caveat is that we cannot be certain that X-ray flux history over the past 33 years reflects the behavior over the last 10,000 years.

We can use the Brown, Bildsten & Rutledge (1998) theory to predict the recurrence time for outbursts of XTE J2123–058, assuming that the outbursts are similar. Using $L = \epsilon \dot{M} c^2$ and the expression relating L_q to the time-averaged mass accretion rate, $L_q = 9 \times 10^{32} \langle \dot{M} \rangle_{-11} \text{ ergs s}^{-1}$, one obtains (see also Wijnands et al. 2001) $L_q = [t_{\text{outburst}} / (t_{\text{outburst}} + t_q)] (\langle L_{\text{outburst}} \rangle / 130)$. Here, t_q is the average time the source spends in quiescence between outbursts, $\langle L_{\text{outburst}} \rangle$ is the average luminosity during an outburst, and t_{outburst} is defined above. For XTE J2123–058, we used the *RXTE*/ASM light curve shown in Figure 3d to determine that the mean 1.5–12 keV count rate during the 40 days (t_{outburst}) between MJD 50,990 and MJD 51,030 was 3.2 s^{-1} , corresponding to $\langle L_{\text{outburst}} \rangle = 1.1 \times 10^{37} \text{ ergs s}^{-1}$ for $d = 8.5 \text{ kpc}$. From the luminosity upper limit of $L_q < 1.4 \times 10^{32} \text{ ergs s}^{-1}$, we obtain a lower limit on the recurrence time, $t_{\text{outburst}} + t_q$, of 67 years. The known outburst history of XTE J2123–058, one outburst in 33 years, assuming that no outbursts were missed, is consistent with these long predicted recurrence times. However, if the recurrence time is in fact shorter than 67 years, then a

mechanism of enhanced cooling of the core would be necessary. The most often mentioned mechanism is neutrino cooling of the core due to the direct Urca process, and this mechanism requires a neutron star with a mass higher than 1.7–1.8 M_{\odot} (Colpi et al. 2001). The mass of the neutron star in XTE J2123–058 has been measured at $1.5 \pm 0.3 M_{\odot}$ or 1.04–1.56 M_{\odot} , so that the mass would have to be at the upper end of the error range for the direct Urca process to operate.

While we have been focusing primarily on the implications of the upper limit on the temperature and luminosity of the thermal component, it is notable that the power-law fit to the spectrum of XTE J2123–058 also indicates that its X-ray luminosity, at $(9_{-3}^{+4}) \times 10^{31} \text{ ergs s}^{-1}$ in the unabsorbed 0.3–8 keV band, is among the lowest for neutron star SXTs. The quiescent luminosity of SAX J1810.8–2609, $\approx 1 \times 10^{32} \text{ ergs s}^{-1}$ (Jonker, Wijnands & van der Klis 2004), is essentially the same as for XTE J2123–058, and the only other system in this class known to have a lower quiescent X-ray luminosity, SAX J1808.4–3658, is also the only millisecond X-ray pulsar system for which there is a measurement of its quiescent X-ray spectrum. The *XMM-Newton* spectrum of SAX J1808.4–3658 is well described by a power-law with $\Gamma = 1.5$ and a 0.5–10 keV unabsorbed luminosity of $5 \times 10^{31} \text{ ergs s}^{-1}$, and the upper limit on the contribution from a thermal component is 10% of the total X-ray luminosity (Campana et al. 2002). If the spectrum of XTE J2123–058 consists of only a power-law component, then its $\Gamma = 3.1_{-0.6}^{+0.7}$ is quite a bit softer than that of SAX J1808.4–3658, and the difference would have to be explained. On the other hand, if the spectrum for XTE J2123–058 consists of a thermal component and a power-law, then its power-law could have the same slope as SAX J1808.4–3658. Concerning the SAX J1808.4–3658 thermal component, Campana et al. (2002) conclude that enhanced neutron star cooling is required to obtain a quiescent luminosity as low as the *XMM-Newton* upper limit implies. However, as mentioned above, such conclusions depend on the assumption that the recent outburst behavior is indicative of the average mass accretion rate over the past 10,000 years.

In summary, our X-ray measurements of XTE J2123–058 in quiescence show that this system is one of the faintest and least luminous of the neutron star SXTs. A comparison of the XTE J2123–058 X-ray properties in outburst and quiescence to that of four other neutron star SXTs that exhibit short outbursts shows that the systems with a higher degree of outburst activity tend to have more luminous thermal components in quiescence, and this is in-line with predictions of the theory of deep crustal heating. For XTE J2123–058, the upper limit on the thermal luminosity is consistent with this theory without requiring enhanced neutron star cooling if the outburst recurrence time is > 67 years, which is consistent with the known outburst history of this source.

JAT would especially like to thank Keith Arnaud for his help with statistical techniques and XSPEC. JAT acknowledges useful conversations with Tariq Shahbaz and Rudy Wijnands. JAT and PK acknowledge partial support from *Chandra* awards GO2-3051X and GO3-4043X issued by the *Chandra* X-ray Observatory Center, which is operated by the Smithsonian Astrophysical Observatory for and on behalf of NASA under contract NAS8-39073. DMG acknowledges support from a CASS postdoctoral fellowship.

REFERENCES

- Brown, E. F., Bildsten, L., & Rutledge, R. E., 1998, *ApJ*, 504, L95
- Campana, S., Colpi, M., Mereghetti, S., Stella, L., & Tavani, M., 1998, *A&A Rev.*, 8, 279
- Campana, S., Israel, G. L., Stella, L., Gastaldello, F., & Mereghetti, S., 2004, *ApJ*, 601, 474
- Campana, S., & Stella, L., 2003, *ApJ*, 597, 474
- Campana, S., et al., 2002, *ApJ*, 575, L15
- Casares, J., Dubus, G., Shahbaz, T., Zurita, C., & Charles, P. A., 2002, *MNRAS*, 329, 29
- Cash, W., 1979, *ApJ*, 228, 939
- Chen, W., Shrader, C. R., & Livio, M., 1997, *ApJ*, 491, 312
- Colpi, M., Geppert, U., Page, D., & Possenti, A., 2001, *ApJ*, 548, L175
- Dickey, J. M., & Lockman, F. J., 1990, *ARA&A*, 28, 215
- Freeman, P. E., Kashyap, V., Rosner, R., & Lamb, D. Q., 2002, *ApJS*, 138, 185
- Greiner, J., Castro-Tirado, A. J., Boller, T., Duerbeck, H. W., Covino, S., Israel, G. L., Linden-Vørnle, M. J. D., & Otazu-Porter, X., 1999, *MNRAS*, 308, L17
- Haensel, P., & Zdunik, J. L., 1990, *A&A*, 227, 431
- Heinke, C. O., Grindlay, J. E., Lloyd, D. A., & Edmonds, P. D., 2003, *ApJ*, 588, 452
- Homan, J., Méndez, M., Wijnands, R., van der Klis, M., & van Paradijs, J., 1999, *ApJ*, 513, L119
- Hynes, R. I., Charles, P. A., Haswell, C. A., Casares, J., Zurita, C., & Serracart, M., 2001, *MNRAS*, 324, 180
- Jonker, P. G., Wijnands, R., & van der Klis, M., 2004, *MNRAS*, 349, 94
- Landolt, A. U., 1992, *AJ*, 104, 340
- Levine, A., Swank, J., & Smith, E., 1998, *IAU Circular*, 6955
- Natalucci, L., Bazzano, A., Cocchi, M., Ubertini, P., Heise, J., Kuulkers, E., in 't Zand, J. J. M., & Smith, M. J. S., 2000, *ApJ*, 536, 891
- Rutledge, R. E., Bildsten, L., Brown, E. F., Pavlov, G. G., & Zavlin, V. E., 1999, *ApJ*, 514, 945
- Rutledge, R. E., Bildsten, L., Brown, E. F., Pavlov, G. G., & Zavlin, V. E., 2001, *ApJ*, 551, 921
- Rutledge, R. E., Bildsten, L., Brown, E. F., Pavlov, G. G., & Zavlin, V. E., 2002a, *ApJ*, 577, 346
- Rutledge, R. E., Bildsten, L., Brown, E. F., Pavlov, G. G., Zavlin, V. E., & Ushomirsky, G., 2002b, *ApJ*, 580, 413
- Shahbaz, T., Zurita, C., Casares, J., Dubus, G., Charles, P. A., Wagner, R. M., & Ryan, E., 2003, *ApJ*, 585, 443
- Soria, R., Wu, K., & Galloway, D. K., 1999, *MNRAS*, 309, 528
- Tavani, M., 1991, *ApJ*, 379, L69
- Tomsick, J. A., Halpern, J. P., Kemp, J., & Kaaret, P., 1999, *ApJ*, 521, 341
- Tomsick, J. A., Heindl, W. A., Chakrabarty, D., Halpern, J. P., & Kaaret, P., 2001, *ApJ*, 559, L123
- Tomsick, J. A., Heindl, W. A., Chakrabarty, D., & Kaaret, P., 2002, *ApJ*, 581, 570
- Wijnands, R., Heinke, C. O., Pooley, D., Edmonds, P. D., Lewin, W. H. G., Grindlay, J. E., Jonker, P. G., & Miller, J. M., 2003a, *astro-ph/0310144*
- Wijnands, R., Homan, J., Miller, J. M., & Lewin, W. H. G., 2003b, *astro-ph/0310612*
- Wijnands, R., Miller, J. M., Markwardt, C., Lewin, W. H. G., & van der Klis, M., 2001, *ApJ*, 560, L159
- Wilson, C. A., Patel, S. K., Kouveliotou, C., Jonker, P. G., van der Klis, M., Lewin, W. H. G., Belloni, T., & Méndez, M., 2003, *ApJ*, 596, 1220
- Zavlin, V. E., Pavlov, G. G., & Shibanov, Y. A., 1996, *A&A*, 315, 141
- Zurita, C., et al., 2000, *MNRAS*, 316, 137

TABLE 1
XTE J2123–058 X-RAY AND OPTICAL OBSERVATIONS

Observatory	UT Date	Energy Band	Exposure Time (s)
<i>BeppoSAX</i>	2000 May 12–13	0.1–10 keV	46,340 ^a
MDM	2000 July 24	Harris <i>R</i>	3 × 600
Lick	2002 September 11	Kron-Cousins <i>R</i>	2 × 700
<i>Chandra</i>	2002 November 13	0.3–8 keV	17,706
MDM	2002 November 25	Harris <i>R</i>	8 × 600

^aThis is the MECS exposure time. The LECS exposure time is 17,080 s.

TABLE 2
SPECTRAL FITS

Model	N_{H}^a (10^{20} cm ⁻²)	Γ	F_{pl}^b (10^{-14} ergs cm ⁻² s ⁻¹)	kT_{bb} (eV)	$L/d_{8.5}^2{}^c$ (10^{32} ergs s ⁻¹)	Fit Quality ^d
pl	$7.0^{+40.0}_{-7.0}$	$3.1^{+2.8}_{-0.8}$	$1.2^{+31.9}_{-0.5}$	—	—	0.69
bb	$0.0^{+40.0}_{-0.0}$	—	—	260^{+50}_{-110}	$0.49^{+2.76}_{-0.12}$	0.97
bb+pl	$8.0^{+38.0}_{-8.0}$	$2.5^{+2.9}_{-2.3}$	$0.70^{+3.67}_{-0.48}$	100^{+130}_{-60}	$0.9^{+160}_{-0.7}$	0.66
pl	6.0	$3.1^{+0.7}_{-0.6}$	$1.1^{+0.5}_{-0.4}$	—	—	0.69
bb	6.0	—	—	240^{+60}_{-50}	$0.63^{+0.22}_{-0.20}$	0.987
bb+pl	6.0	$2.5^{+2.1}_{-2.5}$	$0.7^{+0.5}_{-0.5}$	110^{+180}_{-90}	$0.6^{+36.9}_{-0.5}$	0.64

^aErrors are 90% confidence for all parameters.

^b0.3–8 keV unabsorbed flux. At $d = 8.5$ kpc, $F_{\text{pl}} = 10^{-14}$ ergs cm⁻² s⁻¹ corresponds to 8.6×10^{31} ergs s⁻¹.

^cBolometric luminosity at $d = 8.5$ kpc.

^dFraction of 10,000 simulated spectra for which the C-statistic was better than the C-statistic obtained for the actual spectrum.

TABLE 3
NSA PLUS POWER-LAW FITS

d (kpc)	kT_{eff} (eV)	F_{NSA}^a (10^{-14} ergs cm ⁻² s ⁻¹)	L_{∞}^b (10^{32} ergs s ⁻¹)	Γ	F_{pl}^c (10^{-14} ergs cm ⁻² s ⁻¹)
6	< 57	< 1.1	< 0.80	$2.3^{+1.4}_{-2.5}$	$0.56^{+0.82}_{-0.42}$
8.5	< 66	< 1.1	< 1.4	$2.5^{+1.4}_{-3.1}$	$0.63^{+0.82}_{-0.60}$
11	< 73	< 1.0	< 2.1	$2.8^{+1.9}_{-3.4}$	$0.77^{+0.63}_{-0.77}$

^a0.3–8 keV unabsorbed flux.

^bBolometric luminosity as seen by a distant observer using $4\pi R^2 \sigma T_{\text{eff}}^4 (1 - 2GM/Rc^2)$, where $R = 10$ km and $M = 1.4M_{\odot}$.

^c0.3–8 keV unabsorbed flux. At $d = 8.5$ kpc, $F_{\text{pl}} = 10^{-14}$ ergs cm⁻² s⁻¹ corresponds to 8.6×10^{31} ergs s⁻¹.

TABLE 4
NSA PARAMETERS FOR SHORT OUTBURST FIELD NS SXTs AND X-RAY ACTIVITY

Source ^a	d (kpc)	kT_{eff} (eV)	R (km)	L_{∞}^b (ergs s ⁻¹)	g^c	$\langle \dot{M} \rangle^d$ (M_{\odot} yr ⁻¹)
Aql X-1	5	94–108 ^e	13.2	$(5.3-9.4) \times 10^{33}$	0.828	1.3×10^{-10}
4U 1608–522	3.6	170 ± 30	9.4	5.3×10^{33}	0.748	6.9×10^{-11}
Cen X-4	1.2	76 ± 7	12.9	4.8×10^{32}	0.824	1.9×10^{-11}
SAX J1810.8–2609	4.9	< 72	10	< 2.0×10^{32}	0.765	1.7×10^{-12}
XTE J2123–058	8.5	< 66	10	< 1.4×10^{32}	0.765	2.9×10^{-12}

^aParameters for sources other than XTE J2123–058 are from Rutledge et al. (1999, 2001, 2002a) and Jonker, Wijnands & van der Klis (2004).

^bBolometric luminosity as seen by a distant observer calculated using $4\pi R^2 \sigma T_{\text{eff}}^4 g^2$.

^c $g = \sqrt{1 - 2GM/Rc^2}$ assuming $M = 1.4M_{\odot}$.

^dThe time-averaged mass accretion rate over the past 33 years, estimated according to $\langle \dot{M} \rangle = s \bar{L}_{\text{peak}} N$, where $s = 1.1 \times 10^{-23}$ s² cm⁻² (see Equation 1).

^eThe range of values found in three separate *Chandra* observations.